PD-L1 negatively regulates CD4+CD25+Foxp3+ Tregs by limiting STAT-5 phosphorylation in patients chronically infected with HCV

Debora Franceschini,[1] Marino Paroli,[1] Vittorio Francavilla,[1] Melissa Videtta,[1] Stefania Morrone,[2] Giancarlo Labbadia,[3] Antonella Cerino,[4] Mario U. Mondelli,[4] and Vincenzo Barnaba[1,5]

[1]Dipartimento di Medicina Interna, Fondazione Andrea Cesalpino, [2]Dipartimento di Medicina Sperimentale, and [3]Dipartimento di Clinica e Terapia Medica Applicata, Sapienza Università di Roma, Rome, Italy. [4]Laboratori Sperimentali di Ricerca, Area Infettivologica, Dipartimento di Malattie Infettive, IRCCS Policlinico San Matteo and Università di Pavia, Pavia, Italy. [5]Istituto Pasteur–Cenci Bolognetti, Sapienza Università di Roma, Rome, Italy.

CD4+CD25+Foxp3+ Tregs suppress autoimmune responses. In addition, they limit T cell responses during chronic infection, thereby minimizing T cell–dependent immunopathology. We sought to investigate how Tregs are regulated in the livers of patients chronically infected with HCV, where they control the balance between an adequate protective immune response and suppression of immunopathology. We found that, despite accumulating and proliferating at sites of infection in the livers of patients chronically infected with HCV, Tregs were relatively less expanded than CD4+CD25+Foxp3− effector T cells. The relative lower expansion of intrahepatic Tregs coincided with their upregulation of programmed death–1 (PD-1). PD-1 expression inversely correlated with both Treg proliferation and clinical markers of immune suppression in vivo. Consistent with the possibility that PD-1 controls Tregs, blockade of the interaction between PD-1 and programmed death–1 ligand 1 (PD-L1) enhanced the in vitro expansion and function of Tregs isolated from the livers of patients chronically infected with HCV. Blockade of the interaction between PD-L1 and B7.1 also improved the proliferation of these cells. Interestingly, both PD-1 and phosphorylated STAT-5 were overexpressed in intrahepatic Tregs in a parallel fashion in steady disease conditions, and in an alternate-fluctuating fashion during the course of severe hepatitis reactivation. Notably, PD-L1 blockade upregulated STAT-5 phosphorylation in Tregs ex vivo. These data suggest that PD-L1 negatively regulates Tregs at sites of chronic inflammation by controlling STAT-5 phosphorylation.

Introduction

CD4+CD25+Foxp3+ Tregs are essential in maintaining peripheral immunological self tolerance (1–11). Natural Tregs develop intrathymically in response to specific combinations of TCR and costimulatory signals and represent about 5%–15% of peripheral CD4+ T cells, whereas adaptive Tregs are generated extrathymically from conventional CD4+ T cells, acquiring CD25, Foxp3, and suppression function in response to appropriate stimuli (1–11). Tregs require TCR engagement to nonspecifically suppress via various mechanisms, including cell-cell contact by only partially identified membrane molecules, suppressive cytokine production, and dominant adsorption of IL-2 by high CD25 expression ($CD25^{hi}$) (1–13). Although several biomarkers have previously been determined to be useful in defining Tregs in different physiological or pathological conditions (14–17), the discovery of Foxp3 represented a milestone in the identification of Tregs, because it has been related to the development and suppression function of these cells (4–6). In addition, Foxp3 seems to determine critical molecular patterns of Tregs, including anergy and the incapacity to produce IL-2 or other survival cytokines (18–21). The overexpression of IL-2 receptor (IL-2R) may compensate for this defect by adsorbing high amounts of paracrine IL-2, essential for Treg proliferation (22–24). Absent or decreased Foxp3 expression evolves into different scenarios, ranging from X-linked massive multiorgan autoimmunity (25–27) to impaired suppression function observed in various human and experimental autoimmune disorders (28–31).

Apart from their role in controlling autoimmunity, Tregs seem to perform a critical task in curtailing harmful responses associated with chronic infections (32). Indeed, high Foxp3 expression has been related to the control of immunopathology established by a wide array of persistent pathogens (32). In particular, Tregs have been proposed to participate in the establishment of a fine equilibrium between immunopathology and immune protection, ultimately resulting in long-lasting survival of the host during chronic infections. However, it is unclear how Tregs fine-tune this balance, thus enabling the control of excessive immunopathology without completely suppressing the protective immune responses.

An additional mechanism limiting effector T cell (Teff) responses is related to the propensity of activated T cells to overexpress the programmed death 1 (PD-1) receptor (33, 34). PD-1 can bind both programmed death–1 ligand 1 (PD-L1), which is upregulated on a wide variety of hematopoietic and nonhematopoietic cells, and PD-L2, which is only upregulated on DCs, macrophages, and cultured bone marrow mast cells (33, 34). Upon the simultaneous engagement of PD-1 and B or T cell anti-

Conflict of interest: The authors have declared that no conflict of interest exists.

Nonstandard abbreviations used: CTLA-4, CTL-associated antigen 4; HAI, histological activity index; HD, healthy donor; IHL, intrahepatic lymphocyte; IL-2R, IL-2 receptor; PD-1, programmed death–1; PD-L1, programmed death–1 ligand 1; Teff, effector T cell; Tresp, responder T cell.

Citation for this article: *J. Clin. Invest.* **119**:551–564 (2009). doi:10.1172/JCI36604.

gen-specific receptors to their respective ligands, the cytoplasmic domain–associated immunoreceptor tyrosine-based inhibitory motif of PD-1 is phosphorylated and recruits a series of Src homology 2–containing tyrosine phosphatases (SHPs), leading to the dephosphorylation of the TCR- or BCR-associated effector molecules (33, 34). The inhibitory PD-1/PD-L1 pathway has previously been demonstrated to inhibit both microbial and self-reactive T cell responses and thus to participate in the establishment of chronic infections on the one hand or self tolerance on the other (33–43). In addition, both PD-1 and PD-L1 have been demonstrated to be expressed on Tregs, but whether they influence Treg function is unknown (34, 44–46).

To investigate the roles of Tregs, PD-1 expression, and the possible interplay between their functions in the establishment of long-lasting inflammatory diseases, we studied chronic HCV infection, which is known to establish a lifelong disease in the majority of infected individuals (47, 48). Here, we provide evidence suggesting that a negative regulatory mechanism (referred to herein as contraregulatory) takes place at the level of chronic inflammatory sites via PD-1 overexpression that controls the phosphorylation of STAT-5 in Tregs.

Results

Accumulation and proliferation of Tregs and Teffs in HCV-infected liver. First, Tregs were identified in PBLs isolated from 65 patients with chronic HCV infection and 30 healthy donors (HDs) as well as in intrahepatic lymphocytes (IHLs) isolated from liver biopsies of 57 of the 65 HCV patients studied. PBLs isolated from HDs are referred to herein as HD-PBLs, and cell populations isolated from HCV patients are referred to as HCV-PBLs and HCV-IHLs. $CD4^+CD25^+$ T cells appeared markedly more accumulated at the intrahepatic than at the peripheral level (Figure 1, A and B). More importantly, both the absolute number of $CD4^+CD25^+Foxp3^+$ Tregs and their level of Foxp3 expression were significantly higher in HCV-IHLs than in either HCV-PBLs or HD-PBLs (Figure 1, A, C, and D). Likewise, the number of $CD4^+CD25^+Foxp3^-$ Teffs was significantly higher in IHLs than in PBLs (Supplemental Figure 1; supplemental material available online with this article; doi:10.1172/JCI36604DS1). However, the relative percentage of $Foxp3^+$ cells, compared with that of $Foxp3^-$ cells, was significantly lower in the intrahepatic than in the peripheral $CD4^+CD25^+$ T cells in all HCV patients studied (Figure 1, A and E). Intrahepatic $CD4^+CD25^+Foxp3^-$ T cells were bona fide Teffs because they alone — none of the other intrahepatic or peripheral $CD4^+$ T cell subsets (including Tregs) — expressed significant amounts of IL-2 ex vivo when IHLs were stimulated for 6–8 h with a combination of mAbs to CD3 and CD28 conjugated to Dynabeads (anti-CD3/CD28; Figure 2, A and B). Both the percentage of IL-2^+ Teffs (Figure 2, A and B) and their level of IL-2 mean fluorescence intensity (MFI; data not shown) were significantly higher in IHLs than in PBLs, which suggests that memory effector cells with the highest functional potentiality are recruited in the inflamed tissues. The finding that virtually all the IHLs producing IL-2 were $Foxp3^-$ (Figure 2, A and B) argues against the possibility that the intrahepatic Foxp3 upregulation was the result of a transient, nonfunctional expression by Teffs infiltrating the inflamed liver (49). To investigate whether the intrahepatic Treg accumulation reflected recruitment or increased proliferation, we enumerated Tregs expressing the proliferation marker Ki67 in fresh HCV-IHLs and HCV-PBLs. In comparison to intrahepatic $CD4^+CD25^-Foxp3^-$ T cells or peripheral Tregs, a considerable proportion of intrahepatic $Foxp3^+$ Tregs overexpressed Ki67, albeit to a significantly lesser extent than did intrahepatic $CD4^+CD25^+Foxp3^-$ Teffs (Figure 2, C and D).

Relationship among intrahepatic $Foxp3^+$ cells, suppression function, and chronic disease progression. To examine Treg function in vitro, highly purified peripheral $CD4^+CD25^-Foxp3^-$ responder T cells (Tresps) (50) were labeled with CFSE and stimulated with anti-CD3/CD28 for 6 d in the presence or absence of highly purified unlabeled intrahepatic Tregs, peripheral Tregs, or $CD4^+CD25^-Foxp3^-$ T cells (control cells; Figure 3A). Because of the paucity of IHLs recovered from a single biopsy (no more than 1×10^5 cells), intrahepatic Tregs used in the suppression assay were purified from pooled HCV-IHLs isolated from 3–4 liver biopsies from a total of 16 patients (51). Both intrahepatic (Figure 3B) and peripheral $Foxp3^+$ Tregs (data not shown), but not control $Foxp3^-$ cells (data not shown), efficiently performed suppression function, as detected by the CFSE dilution of Tresps (Figure 3B). The suppression was exerted via a cell-cell contact mechanism (52), as it was inhibited by the separation of Tresps and Tregs in a transwell plate system (Figure 3B). Intrahepatic $Foxp3^+$ cell frequencies were directly related to the suppression function (Figure 3C), but inversely correlated with the expression of Ki67 in intrahepatic Teffs and Tregs (Figure 3, D and E). In addition, intrahepatic $Foxp3^+$ cells correlated with the clinical consequences of the immune suppression, demonstrated by the rise of plasma viremia (Figure 3F) and the decline of hepatic damage (Figure 3G), as calculated by the histological activity index (HAI) score (53). This finding is clearly different from a previous immune histochemistry description showing that increased inflammation directly correlated with increased Tregs in the liver (54). This disparity is likely attributable to the different systems used. Immune histochemistry can detect more precisely the localization of $Foxp3^+$ cells in the different liver areas and is a preferential system to visualize the inflammatory scenario in situ, but it is less sensitive than flow cytometry assay, particularly in multiple staining assays. $Foxp3^+$ cell frequencies did not correlate with Ki67 expression, viral load, or HAI score at the peripheral level (data not shown). In addition, purified intrahepatic and peripheral $CD4^+CD25^+$ cells did not significantly differ in their capacity to perform suppressor function, despite the lower percentage of $Foxp3^+$ cells in the former (Figure 1, A and E). This finding is likely due to the higher level of Foxp3 expression in intrahepatic than in peripheral $CD4^+CD25^+$ cells (Figure 1D), which may compensate for the lower percentage of $Foxp3^+$ cells in the liver (Figure 1E).

Upregulation of PD-1 on intrahepatic Tregs and correlation with disease progression. To determine why intrahepatic Treg expansion and proliferation were constantly lower than intrahepatic Teff expansion in vivo (Figure 1E and Figure 2, C and D), we first examined the expression of the inhibitory PD-1 molecule on both HCV-PBL and HCV-IHL T cell populations from 31 of the 65 HCV patients studied (33, 34). In agreement with previous studies (42, 43), PD-1 was upregulated on activated $CD4^+$ or $CD4^-$ $CD25^+Foxp3^-$ Teffs derived from HCV-infected livers compared with the expression of PD-1 by peripheral Teffs of PBLs derived from HDs or HCV patients (HD-PBLs or HCV-PBLs, respectively; Supplemental Figure 2, A–D). However, more important in the context of this study is the finding that Tregs overexpressed PD-1 to a significantly higher extent than did activated Teffs in both HCV-IHLs and HCV-PBLs in all patients studied (Figure 4, A–C). In addition, HCV-IHL Tregs upregulated PD-1 significantly more than did HCV-PBL or HD-PBL Tregs (Figure 4, A–C, and Supplemental Figure 3, A

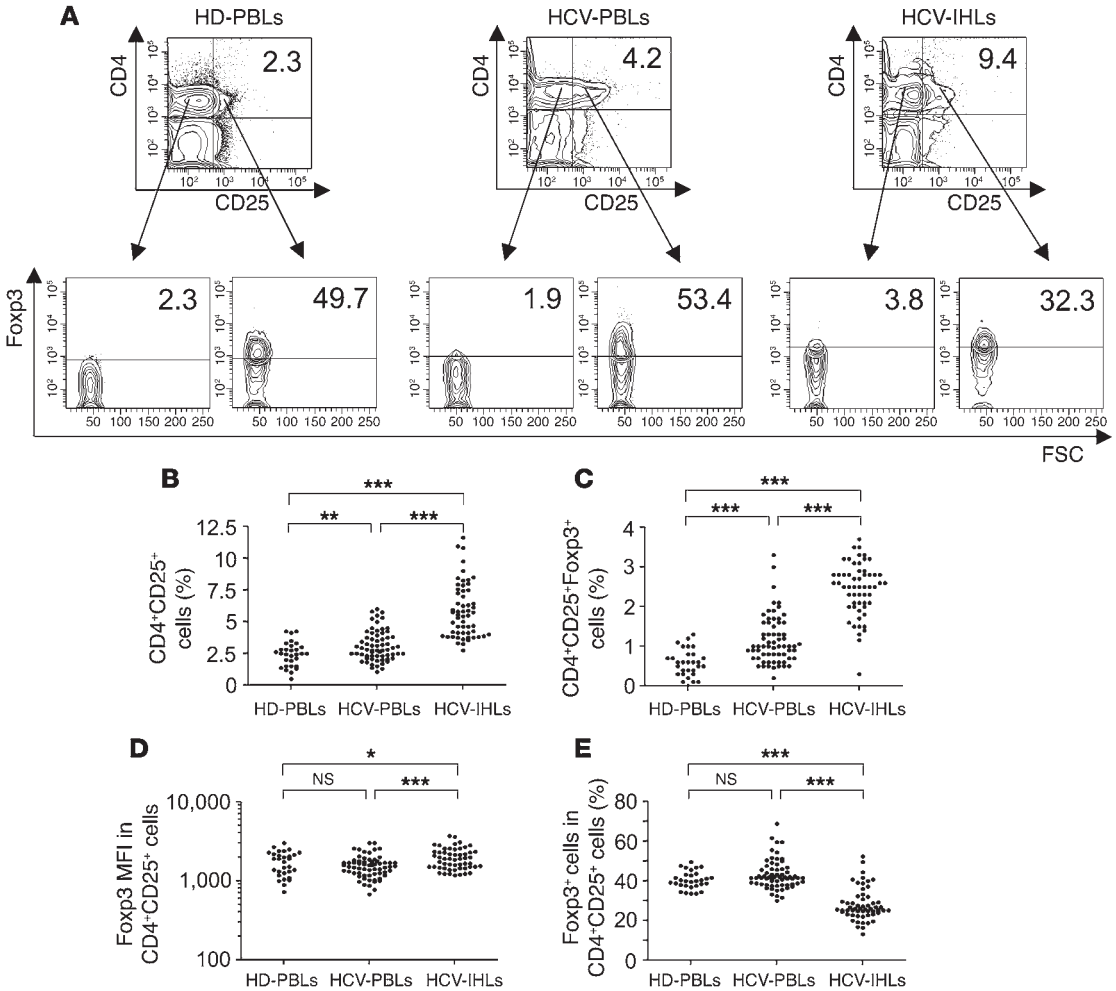

Figure 1

Treg and Teff repertoire in liver and peripheral blood of HCV patients. (**A**) Representative flow cytometry analyses of HD-PBLs, HCV-PBLs, or HCV-IHLs stained with mAbs to CD4, CD25, and Foxp3. The percentage of cells is indicated in each quadrant. FSC, forward scatter. (**B**) Percentage of CD4$^+$CD25$^+$ cells in HD-PBLs, HCV-PBLs, and HCV-IHLs. (**C**–**E**) Percentage of CD4$^+$CD25$^+$Foxp3$^+$ cells (**C**), MFI of Foxp3$^+$ cells in CD4$^+$CD25$^+$ cells (**D**), and relative percentage of Foxp3$^+$ cells in CD4$^+$CD25$^+$ cells (**E**) from HD-PBLs, HCV-PBLs, and HCV-IHLs. In **B**–**E**, statistical analyses of values between HCV-IHLs and HCV-PBLs were performed with the nonparametric Mann-Whitney *U* test for paired data, whereas those between cell populations from HCV patients and HDs were performed with the nonparametric Mann-Whitney *U* test for unpaired data.*$P < 0.05$; **$P < 0.009$; ***$P < 0.0015$. Each symbol represents a single individual.

and B). Importantly, the ratio between the PD-1$^+$ and Foxp3$^+$ Treg percentages (PD-1/Foxp3 cell ratio) infiltrating the liver of HCV patients correlated inversely with the viral load (Figure 4D) and directly with the HAI score (Figure 4E), thus indicating that PD-1 on Tregs restrains the Foxp3-related suppression of both antiviral and immunopathology-related responses. No correlation among the parameters was shown at the level of the peripheral T cell populations (data not shown).

Enhanced IL-2–dependent proliferation of HCV-specific Tregs by PD-L1 blockade. To determine the functional capacity of PD-1 expression, we first selected HCV-PBL samples with abundant expression of PD-1 (Figure 4) and purified both Tregs and Tresps that were stained or not with CFSE. After 6 d of stimulation, CFSE-labeled Tresps proliferated in response to either antigenic stimulus, with autologous APCs pulsed with both HCV-NS3 and HCV-core antigens (HCV-Ags/APCs; Figure 5A), or nonspecific stimulus, with anti-CD3/CD28 (data not shown), and an even higher extent of proliferation was observed in the presence of a blocking anti–PD-L1 mAb (Figure 5A). Even in the presence of anti–PD-L1 mAb, less than 1% of these cells became Foxp3$^+$ (Figure 5A), which supports the in vivo evidence suggesting that Foxp3 expression was not the result of a transient, nonfunctional expression by Teffs in our model (Figure 2, A and B, and ref. 49). Cumulative experiments with purified Tresps from a total of 9 HCV patients confirmed that PD-L1 blockade resulted in a significant increase of HCV-specific T cell proliferation compared with isotype control treatment (Figure 5B), thus highlighting the recently observed role of PD-1 in the exhaustion of Teffs during chronic infections (36–43).

Next, we assessed the effect of PD-L1 blockade on the expansion of Tregs. Consistent with the finding that Tregs are anergic in vitro (8), CFSE-labeled Tregs were unable to proliferate after 6 d of contact with antigenic (Figure 6A) or nonspecific stimulus (data not shown) or when cultured in a transwell plate system, in

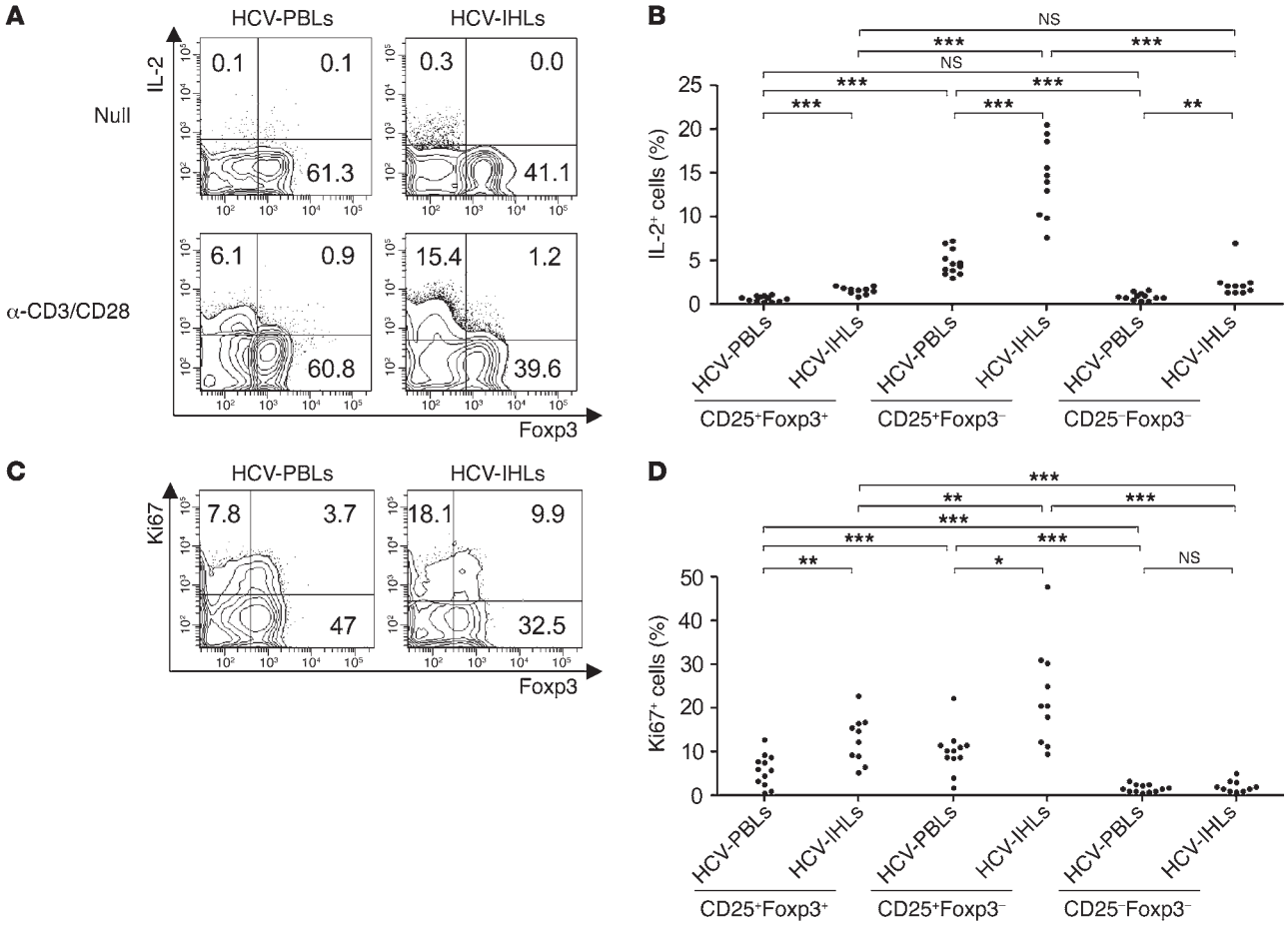

Figure 2

Degree of difference in IL-2 production and proliferation between Tregs and Teffs in the site of infection. (**A**) Representative flow cytometry analysis of HCV-PBLs or HCV-IHLs stained with mAbs to CD4, CD25, and Foxp3, stimulated or not with anti-CD3/CD28, and processed to detect intracellular IL-2. Contour plot analyses are gated on CD4+CD25+ cells and show percentages of double-stained IL-2+Foxp3+ cells. The percentage of cells is indicated in each quadrant. (**B**) Percentage of IL-2+ cells (analyzed by flow cytometry as in **A**) in peripheral or intrahepatic cell populations. Values subtracted the background are shown. (**C**) Representative flow cytometry analysis of HCV-PBLs or HCV-IHLs stained with mAbs to CD4, CD25, Foxp3, and Ki67. Contour plot analyses are gated on CD4+CD25+ cells and show cells stained with mAbs to Ki67 and Foxp3. The percentage of cells is indicated in each quadrant. (**D**) Percentage of Ki67+ cells (analyzed by flow cytometry as in **C**) in peripheral or intrahepatic cell populations. In **B** and **D**, statistical analyses of values between HCV-IHLs and HCV-PBLs were performed with the nonparametric Mann-Whitney *U* test for paired data, whereas those between cell populations from HCV patients and HDs were performed with the nonparametric Mann-Whitney *U* test for unpaired data. $^{*}P < 0.05$; $^{**}P < 0.0065$; $^{***}P < 0.0015$. Each symbol represents a single individual.

which they were seeded with the antigenic stimulus in the lower wells and unstimulated Tresps were cultured in the upper wells (Figure 6A). However, Tregs were rescued from anergy and efficiently proliferated, as demonstrated by the substantial expansion of Foxp3+ cells when Tregs and Tresps were independently stimulated in the separated transwell plates (i.e., Tregs stimulated with HCV-Ags/APCs and Tresps stimulated with anti-CD3/CD28; Figure 6A). Conversely, Tregs remained anergic when an anti–IL-2 mAb was added to the wells containing the stimulated Tresps, suggesting that IL-2 produced by Tresps plays a major role in the expansion of Tregs (Figure 6A). The antigen specificity of Foxp3+ Tregs was highlighted by the evidence that their antigen-driven expansion was consistently inhibited by the addition of anti–MHC class II mAb, but not anti–MHC class I mAb, to the wells containing Tregs (Figure 6A). The addition of anti–PD-L1 mAb to cultures containing Tregs alone in the presence of HCV-Ags/APCs or anti-CD3/CD28 was unable to rescue Tregs from anergy in vitro (Figure 6B), even though these cells expressed both PD-1 (Figure 4) and PD-L1 (data not shown). On the contrary, the expansion of intrahepatic CD25+Foxp3+ Tregs in response to the combination of the antigenic stimulus and either autologous IL-2–producing Tresps or soluble IL-2 substantially improved with PD-L1 blockade compared with culture conditions in the absence of anti–PD-L1 (Figure 6B). Similar results were obtained by stimulating Tregs with anti-CD3/CD28 and IL-2 in the presence of anti–PD-L1, which suggests that Tregs can suppress each other via the PD-1/PD-L1 interaction (data not shown). Cumulative experiments with Tregs from a total of 8 HCV patients showed that PD-L1 blockade resulted in a significant increase in IL-2–dependent, HCV-specific Treg proliferation compared with treatment with isotype control (Figure 6C). Similar results were obtained by using intrahepatic Tregs purified from a pool of IHLs that in turn had been isolated

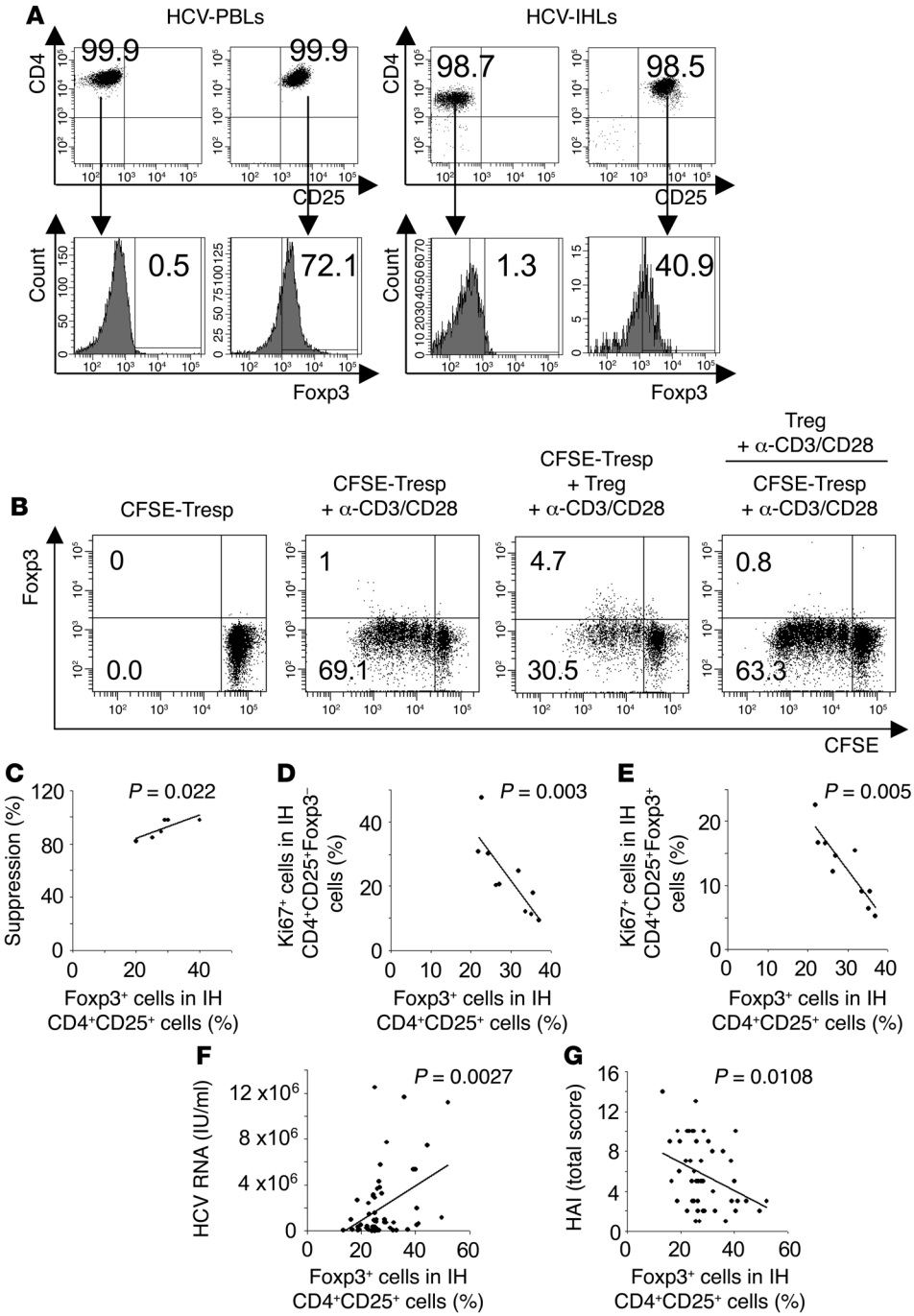

Figure 3

Intrahepatic Foxp3+ Tregs are related to suppression function and disease progression. (**A**) Representative analysis of highly purified CD4+CD25− or CD4+CD25+ HCV-PBLs or HCV-IHLs stained with mAbs to CD4, CD25, and Foxp3. Numbers represent the percentage of stained cells. (**B**) Single representative suppression function experiment of 6, in which CFSE-labeled Tresps from an HCV patient were cultured alone or cocultured with CD4+CD25+ Tregs previously purified from pooled HCV-IHLs derived from liver biopsies of 4 patients. Cells were cultured or cocultured either in the same well or in separated transwell plate system (denoted by line) in the presence of anti-CD3/CD28. After 6 d, cells were stained with labeled mAbs to CD4, CD25, and Foxp3. The percentage of cells is indicated in each quadrant. (**C**) Correlation between suppression function, calculated as percent of suppression by 6 pools of Tregs isolated from 3–4 independent liver biopsies of a total of 16 HCV patients, and mean percentage of Foxp3+ cells in the corresponding intrahepatic (IH) CD4+CD25+ cells. (**D** and **E**) Correlation between percentage of intrahepatic Foxp3+ cells and of Ki67+ cells in intrahepatic Teffs (**D**) and Tregs (**E**). (**F** and **G**) Correlation between percentage of intrahepatic Foxp3+ cells and viral load (**F**) or HAI (**G**). In **C**–**G**, statistical analyses were performed using Pearson's correlation test. Each symbol represents 1 pool of intrahepatic Tregs from 3–4 patients (**C**) or a single individual (**D**–**G**).

from 3 independent liver biopsies (data not shown). To investigate whether the inhibitory PD-1 effect on Treg proliferation accounts for the inverse correlation we observed between Foxp3+ and Ki67+ Tregs in vivo (Figure 3, D and E), we sorted PD-1+ and PD-1− Tregs from purified CD4+CD25+Foxp3+ cell populations. Under conditions in which cells were stimulated for 6 d with anti-CD3/CD28 and IL-2 in the presence of anti–PD-L1, a considerable increase in Ki67+ cells was shown in the PD-1+ Treg population, but not in the PD-1− Treg population (Supplemental Figure 4). Control experiments revealed that the anti–PD-1 mAb used for cell sorting in this as well as the following experiments did not interfere with the PD-1/PD-L1 interaction. Indeed, proliferation of CFSE-stained Foxp3+ cells in response to anti-CD3/CD28 and IL-2 was not affected by the addition of anti–PD-1 (data not shown). These data suggest that this anti–PD-1 antibody recognizes a sequence that seems not involved in the PD-1/PD-L1 interaction. On the other hand, the evidence that B7.1 was overexpressed, although at a level consistently less than that of PD-1, on both fresh intrahepatic Tregs and in vitro–activated Tregs (Supplemental Figure 5, A and B) led us to investigate whether the inhibitory effect by PD-L1 on Treg proliferation might be mediated, at least in part, by interaction with B7.1 (55). Consistent with this possibility, blocking of PD-L1/B7.1 inter-

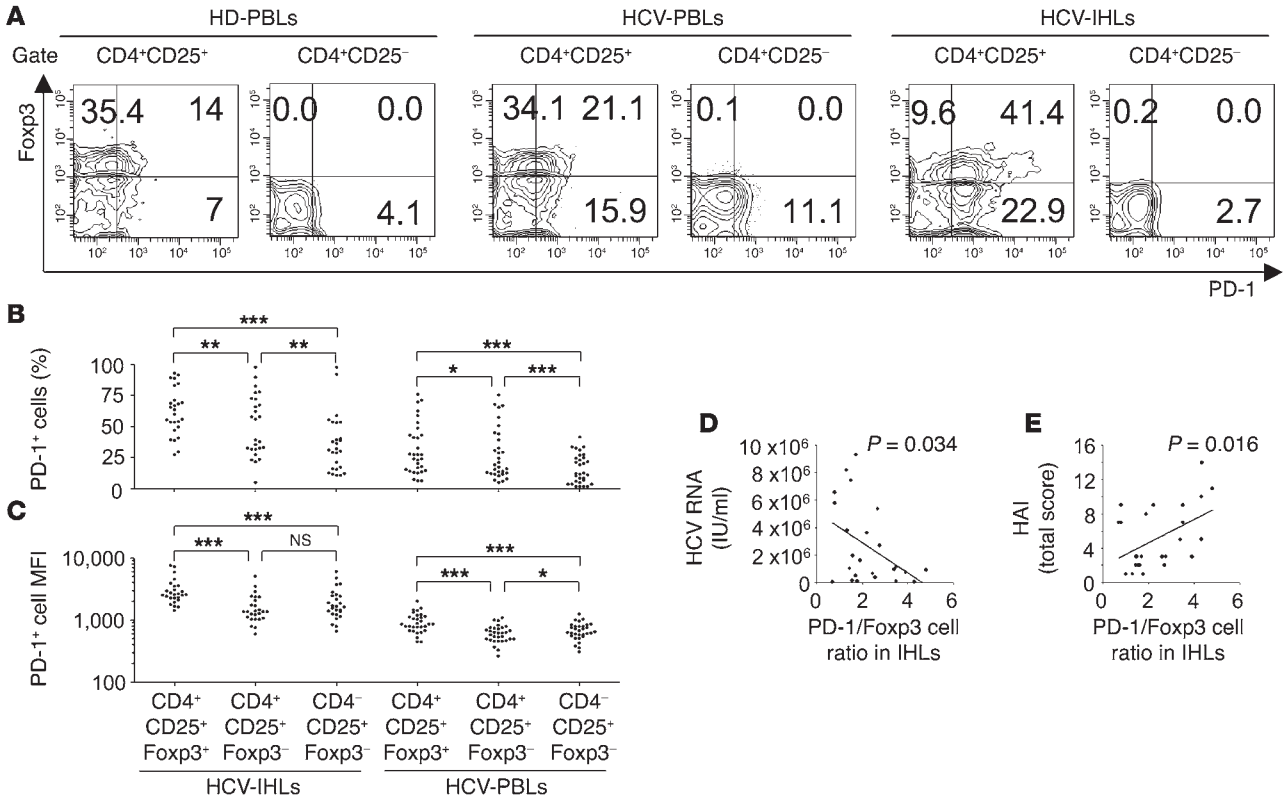

Figure 4

PD-1 upregulation on Tregs contrabalances the Foxp3 correlation with the disease progression. (**A**) Representative flow cytometry analyses of HD-PBLs, HCV-PBLs, and HCV-IHLs stained with mAbs to CD4, CD25, Foxp3, and PD-1. Contour plot analyses are gated on $CD4^+CD25^+$ or $CD4^+CD25^-$ cells, and percentages of $Foxp3^+$ and/or $PD\text{-}1^+$ cells are shown in each quadrant. (**B** and **C**) Percentage (**B**) and MFI (**C**) of $PD\text{-}1^+$ cells in cell populations derived from HCV-PBLs or HCV-IHLs. Statistical analyses of values between HCV-IHLs and HCV-PBLs were performed with the nonparametric Mann-Whitney *U* test for paired data, whereas those between cell populations from HCV patients and HDs were performed with the nonparametric Mann-Whitney *U* test for unpaired data. $^*P < 0.03$; $^{**}P < 0.0075$; $^{***}P < 0.0001$. (**D** and **E**) Correlation between PD-1/Foxp3 cell ratio in IHLs and viral load (**D**) or HAI (**E**). Statistical analyses were performed using Pearson's correlation test. Each symbol represents a single individual.

action with a soluble form of CTL-associated antigen 4 (CTLA-4) via the use of a fusion CTLA-4/Ig protein that binds B7.1 with high affinity (56) improved Treg proliferation in response to anti-CD3/CD28 and IL-2 in vitro (Supplemental Figure 6, A and B). However, anti–PD-L1 improved Treg proliferation consistently more than did CTLA-4/Ig (Supplemental Figure 6, A and B).

Enhanced expansion and suppression of Tregs by PD-L1 blockade. Next we investigated whether the enhanced expansion of Tregs by PD-L1 blockade correlated with the increased suppression function. Under conditions in which purified CFSE-labeled $CD4^+CD25^+$ Tregs were stimulated with anti-CD3/CD28 in the presence of IL-2 and the mAb to PD-L1 or isotype control for 6 d of culture, PD-L1 blockade was confirmed to upregulate the $Foxp3^+$ cell proliferation, compared with the Tregs stimulated in the presence of the isotype control (Figure 7A). Importantly, a marked suppression of the CFSE-labeled Tresp proliferation in response to anti-CD3/CD28 was highlighted when the cells were cocultured with Tregs demonstrating substantial expansion of $Foxp3^+$ cells after previous stimulation in the presence of anti–PD-L1 mAb compared with suppression by Tregs previously stimulated in the absence of anti–PD-L1 mAb (Figure 7, A and B). On the contrary, sorted, fresh $PD\text{-}1^+$ or $PD\text{-}1^-$ $Foxp3^+$ Tregs without previous stimulation (Supplemental Figure 7A) efficiently suppressed proliferation in a similar fashion, and the PD-L1 blockade did not increase the intrinsic suppression capacity of $PD\text{-}1^+$ Tregs (Supplemental Figure 7B).

PD-L1 inhibition of Treg proliferation via interference with STAT-5 phosphorylation. After determining that the PD-L1 blockade enhanced IL-2–dependent expansion of Tregs, we analyzed the effect of PD-L1 on STAT-5 phosphorylation, known to be implicated in IL-2R signaling (57, 58) and proposed to play a key role in Treg homeostasis (59, 60). STAT-5 appeared to be spontaneously phosphorylated in a notable proportion of all cell populations expressing CD25, significantly more so in the $CD25^{hi}$ than in the $CD25^{lo/-}$ cell subset (Figure 8, A and B). More detailed analyses of $CD25^+$ populations showed that $pSTAT\text{-}5^+$ cells were more highly represented in $Foxp3^+$ Tregs than in $Foxp3^-$ Teffs, particularly in those expressing PD-1 (Figure 8, A and B). In addition, pSTAT-5 was more highly expressed in all populations infiltrating the inflamed liver (Figure 8, A and B) than in those derived from the peripheral blood (Figure 8A and Supplemental Figure 8). To verify that homeostatic interplay between PD-1 and pSTAT-5 expression takes place in vivo, we performed longitudinal analyses in 2 selected patients showing a severe hepatitis reactivation that is generally considered a rare event during chronic HCV infection

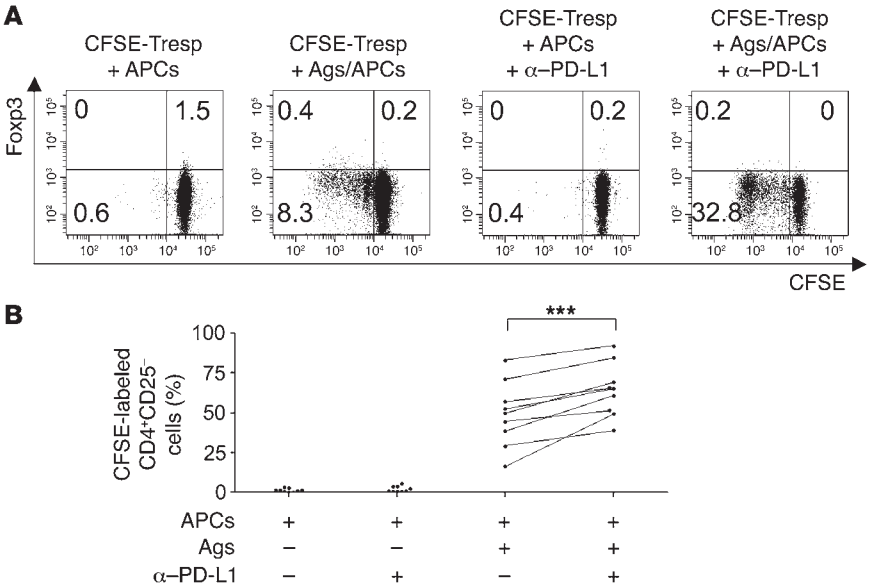

Figure 5

PD-L1 blockade enhances proliferation of HCV-specific Teffs. (**A**) Representative experiment in which CFSE-labeled Tresps from an HCV patient were stimulated with APCs alone or HCV-Ags/APCs, in the presence or absence (isotype control) of anti–PD-L1 mAb. After 6 d, cells were stained with mAbs to CD4, CD25, and Foxp3. Dot plot analyses are gated on $CD4^+CD25^-$ cells and show cells stained with both CFSE and anti-Foxp3. The percentage of cells is indicated in each quadrant. (**B**) All experiments (of which a representative is shown in **A**) showing the percentage of CFSE-labeled Tresps upon antigen stimulation in the presence or absence of anti–PD-L1. Statistical analyses were performed with nonparametric Mann-Whitney *U*-test for paired data. ***$P < 0.0008$. Each symbol represents a single individual.

(61). Interestingly, we observed a peak of both Treg expansion and pSTAT-5 intensity, which followed the raised levels of serum alanine aminotransferase and frequencies of T cells promptly producing IL-2 ex vivo (i.e., disease activity) and preceded a dramatic contraction of disease activity (Figure 8C). Subsequently, both Treg expansion and pSTAT-5 intensity decreased in relation with the upregulation of PD-1, which anticipated the establishment of steady disease activity (Figure 8C). Similarly, PD-1 and pSTAT-5 were overexpressed in Teffs — albeit to a lower extent than in Tregs — by the same patients (data not shown), evidence in support of the parallelism of the Teff and Treg expansions. No correlation between the parameters above and the serum HCV-RNA levels in the kinetic studies was shown. Notably, PD-L1 inhibited STAT-5 phosphorylation in fresh intrahepatic Tregs ex vivo. Indeed, upon 6 h stimulation with anti-CD3/CD28 and IL-2 in the presence of anti–PD-L1 mAb, both $pSTAT\text{-}5^+$ cell expansion and MFI increased to a greater extent in Tregs than in Teffs, and to a greater extent in HCV-IHLs than in HCV-PBLs (Figure 9A, Supplemental Figure 9A, and data not shown) or HD-PBLs (data not shown). Amazingly, pSTAT-5 upregulation was also observed in the $PD\text{-}1^-$ cell populations, albeit to a lesser degree than in the $PD\text{-}1^+$ cell populations (Figure 9A and Supplemental Figure 9A). Therefore, we investigated whether this phenomenon was caused by increased capacity of $PD\text{-}1^+$ cells to provide bystander signals to the $PD\text{-}1^-$ cells after stimulation of the total IHLs or PBLs (containing both $PD\text{-}1^+$ and $PD\text{-}1^-$ cells) in the presence of blocking anti–PD-L1 antibody. This hypothesis was ascertained by experiments in which we used fresh $PD\text{-}1^+$ or $PD\text{-}1^-$ $Foxp3^+$ Tregs (Figure 9B and Supplemental Figure 9B) sorted from HD-PBLs and HCV-PBLs. Under these conditions, pSTAT-5 was upregulated in $Foxp3^+$ Tregs to a much greater extent than in $Foxp3^-$ Teffs, and the addition of anti–PD-L1 mAb caused a consistent increase of pSTAT-5 upregulation in the $PD\text{-}1^+$ Tregs (Figure 9B), but not in the $PD\text{-}1^-$ cells (Supplemental Figure 9). Control experiments revealed that the levels of nonphosphorylated STAT-5, constitutively expressed by all cells, did not change in this experimental setting (data not shown). Importantly, kinetics experiments demonstrated that after IL-2 contact, STAT-5 phosphorylation was notably more rapid, but less vigorous and sustained, in Tresp than in Tregs (Supplemental Figures 10 and 11). In particular, $CD4^+$ Tresps remained both $CD25^-$ and $pSTAT\text{-}5^-$ after 30 minutes of stimulation with anti-CD3/CD28 (Supplemental Figure 10). However, after 1 h of IL-2 culture, the $CD25^+$ cell population demonstrated prompt upregulation of STAT-5 that decreased with time. Conversely, the $CD4^+CD25^{hi}Foxp3^+$ cells, but not the $CD25^{lo}Foxp3^-$ or the tiny $CD25^{lo}Foxp3^+$ populations, displayed pSTAT-5 later, but to a higher extent and more sustained over time, compared with Tresps (Supplemental Figure 11). In addition, the PD-L1 blockade was confirmed to improve pSTAT-5 more so in $PD\text{-}1^+$ Tregs than in $PD\text{-}1^+$ Teffs (data not shown).

Discussion

Our findings suggest that PD-1 expression correlates with the regulation of expansion and suppression capacity of Tregs during chronic HCV infection. We first observed substantial Treg accumulation in the inflamed liver of HCV patients and that some of this accumulation was caused by increased proliferation in vivo, as calculated by Ki67 expression. It will be interesting to study whether Treg proliferation can initiate directly at the site of infection or whether it occurs in the draining lymph nodes, causing divided cells to migrate into the inflamed tissue. Moreover, accumulation and proliferation of Tregs were synchronized with those of Teffs at the site of infection, but at a level significantly and consistently lower than the parallel expansion of Teff IHLs. Nonetheless, intrahepatic Tregs were intrinsically professional, because they exerted efficient suppression function that was directly related with the level of Foxp3 expression, the decline of proliferating ($Ki67^+$) T cells, and the clinical consequences of downregulation of antiviral and immunopathological responses (i.e., increased viral load and decreased HAI score, respectively) in vivo. Because we were able to demonstrate notable production of IL-2 by Teffs derived from inflamed liver, which is known to be the most important source of HCV antigens, the capacity of Tregs to proliferate in vivo is likely caused by the sustained amounts of viral antigens and paracrine IL-2 at the site of infection. The results of our antigen-specific Treg proliferation assay in vitro supported this view because the com-

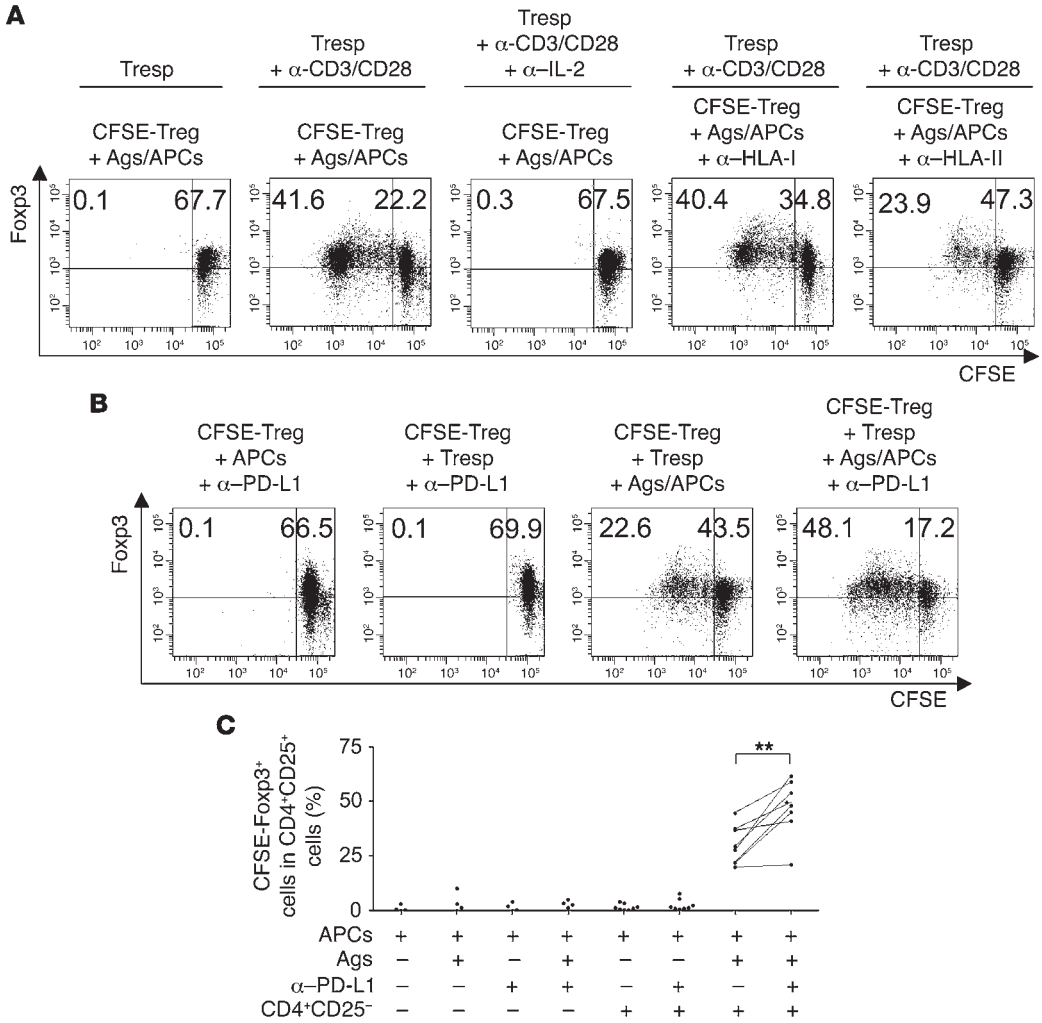

Figure 6

PD-L1 blockade enhances IL-2–dependent proliferation of HCV-specific Tregs. (**A**) Single representative of 5 experiments, in which purified CFSE-labeled CD4+CD25+ Tregs from an HCV patient were stimulated with APCs alone or HCV-Ags/APCs and cocultured in a transwell plate system (denoted by lines) with Tresps that were stimulated or not with anti-CD3/CD28 in the presence or absence of anti–IL-2 mAb. In some cocultures, anti–HLA class I or –HLA class II mAb was added to the wells containing antigen-stimulated Tregs. After 6 d, cells were stained with mAbs to CD4, CD25, and Foxp3. Dot plot analyses are gated on CD4+CD25+ cells and show cells stained with both CFSE and anti-Foxp3. The percentage of cells is indicated in each quadrant. (**B**) Single representative of all the experiments shown in **C**, in which CFSE-labeled Tregs from an HCV patient were stimulated with APCs alone or HCV-Ags/APCs in the presence or absence (isotype control) of anti–PD-L1 mAb and/or Tresps. After 6 d, cells were stained with mAbs to CD4, CD25, and Foxp3. Dot plot analyses are gated on CD4+CD25+ cells and show cells stained with both CFSE and anti-Foxp3. The percentage of cells is indicated in each quadrant. (**C**) Percentage of CFSE-labeled Foxp3+ cells in Tregs upon antigen stimulation in the presence or absence of anti–PD-L1 and/or Tresps. Statistical analyses were performed with nonparametric Mann-Whitney *U* test for paired data. $^{**}P < 0.0040$. Each symbol represents a single individual.

bination of viral antigens and IL-2 efficiently rescued Tregs from anergy in the majority of HCV patients tested, indicating a key role for HCV in the generation of functional Tregs. Further analyses, such as those using class II tetramers (62), are needed to determine whether most Tregs are antigen specific or expand in response to non–antigen-specific stimuli such as inflammation-, necrotic cell–, or virus-derived products.

To understand why the expansion and proliferation of intrahepatic Tregs were, although parallel, constantly less than those of intrahepatic Teffs in all HCV patients tested, we investigated the possibility that Tregs are more susceptible than the effectors to the PD-1–dependent exhaustion mechanism in the inflamed tissue (33, 34). The lower Treg expansion correlated with significantly higher expression of PD-1 on Tregs than on Teffs infiltrating the inflamed liver. Further in vivo experiments revealed that the PD-1/Foxp3 cell ratio correlated inversely with the viral load and directly with the HAI score, which suggests that PD-1 expression on Tregs contraregulates the suppression of both the antiviral and the immunopathological responses. The PD-L1 blockade significantly increased both the expansion and the relative suppression function of Tregs when stimulated with either specific or nonspecific TCR ligands plus paracrine IL-2 in the presence of a blocking mAb to PD-L1 in vitro, thus providing evidence for the hypothesis that the inhibition of suppression is PD-1 dependent.

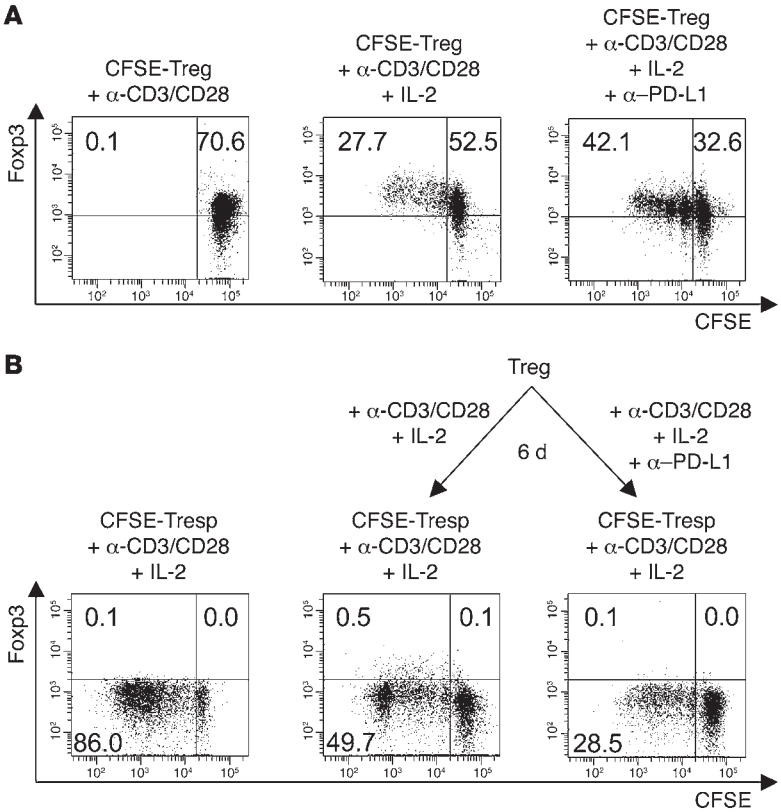

Figure 7

Improved suppression function by PD-L1 blockade is related to Treg expansion. (**A**) Single representative of 4 experiments in which CFSE-labeled CD4$^+$CD25$^+$ Tregs were stimulated with anti-CD3/CD28 in the presence or absence of IL-2 (50 U/ml) or anti–PD-L1. After 6 d, cells were stained with mAbs to CD4, CD25, and Foxp3. Dot plot analyses are gated on CD4$^+$CD25$^+$ cells and show cells stained with both CFSE and anti-Foxp3. The percentage of cells is indicated in each quadrant. (**B**) Single representative of 3 experiments in which CFSE-labeled Tresps were stimulated with anti-CD3/CD28 and 50 U/ml IL-2, alone or in coculture (at a 1:1 cell ratio) with Tregs that had previously stimulated for 6 d with anti-CD3/CD28 and 50 U/ml IL-2 or with anti-CD3/CD28, IL-2, and anti–PD-L1. After 6 d, cells were stained with mAbs to CD4, CD25, and Foxp3. Dot plot analyses are gated on CD4$^+$CD25$^-$ cells and show cells stained with both CFSE and anti-Foxp3. The percentage of cells is indicated in each quadrant.

The potential role of PD-1–dependent control of Treg proliferation is emphasized by the observation that PD-L1 blockade (by anti–PD-L1) increased the expansion of Ki67$^+$ cells in the Treg population upon TCR-dependent stimulation in the presence of IL-2 in vitro. This finding is consistent with the inverse correlation observed between Foxp3$^+$ and Ki67$^+$ Tregs in vivo. Importantly, the interaction of PD-L1 with both PD-1 and B7.1 was involved in controlling Treg proliferation in our system in vitro, supporting the recent identification of human B7.1, but not B7.2, as an additional inhibitory partner for PD-L1 (55). However, blocking with anti–PD-L1 improved Treg proliferation consistently more than did blocking with CTLA-4/Ig, likely because PD-L1 interacts with PD-1 with both higher affinity (55) and higher avidity than it does with B7.1, as indicated by our observation that both in vivo– and in vitro–activated Tregs expressed higher levels of PD-1 than B7.1. Nevertheless, the PD-L1–mediated inhibition of Treg function is dependent on its capacity to decrease expansion, and ultimately the number of Tregs, rather than the intrinsic Treg suppression capacity. This finding is consistent with both the previous finding that Foxp3 expression dictates and fixes the suppression function of the single Tregs regardless of the presence of inhibitory signals (18, 19) and the hypothesis that decreased expansion of Tregs by PD-1 can decrease suppression function in a given inflammatory context. In contrast, the lack of evident correlation when we considered the peripheral Tregs further demonstrates that peripheral immune settings do not necessarily reflect the local immune responses present at a given inflammatory site (51, 63–67).

Tregs overexpress the heterotrimeric IL-2R, consisting of the α (CD25), β, and common γ chains. These chains induce different signaling pathways, including the activation of JAK-3 and the resulting phosphorylation of STAT-5, which then dimerizes, translocates to the nucleus to activate gene transcription, and supports cellular survival and proliferation (57, 58, 68). Herein, we demonstrated that pSTAT-5 was spontaneously overexpressed in intrahepatic Tregs, to a significantly greater extent than in intrahepatic Teffs, and paralleled both CD25^{hi} and PD-1 expression in vivo. In addition, kinetic studies in patients with severe hepatitis reactivation showed that pSTAT-5 and PD-1 expression in Tregs were upregulated in an alternate fashion in vivo: pSTAT-5 upregulation followed the peak and anticipated the dramatic suppression of disease activity, whereas PD-1 upregulation preceded the return of both pSTAT-5 and disease activity to steady levels. Finally, PD-L1 blockade increased both proliferation and pSTAT-5 expression by fresh intrahepatic Tregs significantly more than by intrahepatic Teffs ex vivo. Taken together, these data support the hypothesis that PD-1 controls Treg proliferation by limiting STAT-5 phosphorylation that is likely caused by the capture (via the highly expressed IL-2R) of high amounts of paracrine IL-2 produced by CD25^{lo} Teffs at the site of infection (22–24). The findings that PD-1 is consistently more expressed than B7.1 and that anti–PD-L1 enhanced Treg proliferation more so than CTLA-4/Ig led us to hypothesize that the pSTAT-5 control is likely the result of the PD-L1/PD-1 more than the PD-L1/B7.1 interaction. The potential existence of a homeostatic loop, whereby the upregulation of pSTAT-5 in IL-2–consuming Tregs causes the upregulation of PD-1 that in turn controls STAT-5 phosphorylation via the activation of the SHP2 (33, 58), remains an interesting and relevant issue that requires further study. Our results are consistent with the recent finding supporting dominant IL-2 adsorption by Tregs as a critical mechanism of suppression that results in IL-2 depriva-

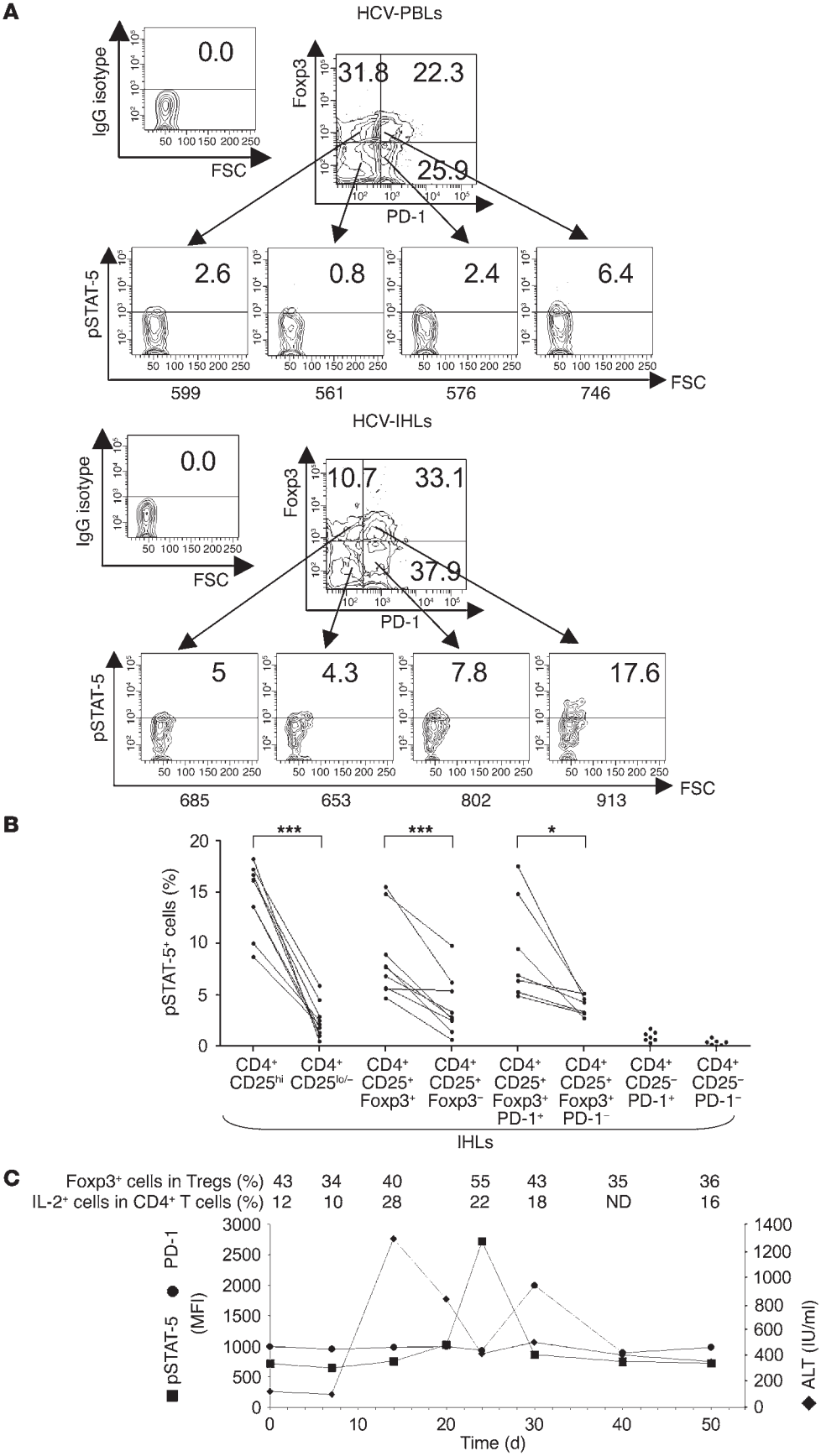

Figure 8

Tregs overexpress pSTAT-5 and PD-1 in a parallel fashion in steady states, but in an alternate fashion during the course of hepatitis reactivation. (**A**) Representative flow cytometry analyses of fresh HCV-PBLs or HCV-IHLs stained with mAbs to CD4, CD25, Foxp3, and PD-1 and (at the intracytoplasmic level) with the polyclonal rabbit anti–pSTAT-5, followed by secondary FITC-conjugated goat anti-rabbit antibody. Contour plot analyses (upper histograms) are gated on CD4+CD25+ cells and show percentages of cells stained with mAbs to PD-1 and Foxp3, whereas analyses in the lower histograms are gated in cells stained with mAbs to PD-1 and Foxp3 and show pSTAT-5+ cells. The counter plot analyses of samples stained with the isotype control of anti–pSTAT-5 are shown above. The percentage of cells is indicated in each quadrant. pSTAT-5 MFI values are shown below the flow cytometry analyses. (**B**) Percentage of intrahepatic pSTAT-5+ cells in the indicated cell populations. Statistical analyses were performed with the nonparametric Mann-Whitney *U* test for paired data. $^{*}P < 0.025$; $^{***}P < 0.0006$. Each symbol represents the value for a single individual. (**C**) Kinetics of pSTAT-5 and PD-1 expression in Tregs (expressed as MFI) in relation to the values of alanine aminotransferase (ALT; normal value, 0–40 IU/ml), percentage of Foxp3+ cells in Tregs, and percentage of IL-2+ cells in CD4+ Teffs, in a representative of 2 patients showing a severe hepatitis reactivation. Similar results were obtained in the second patient.

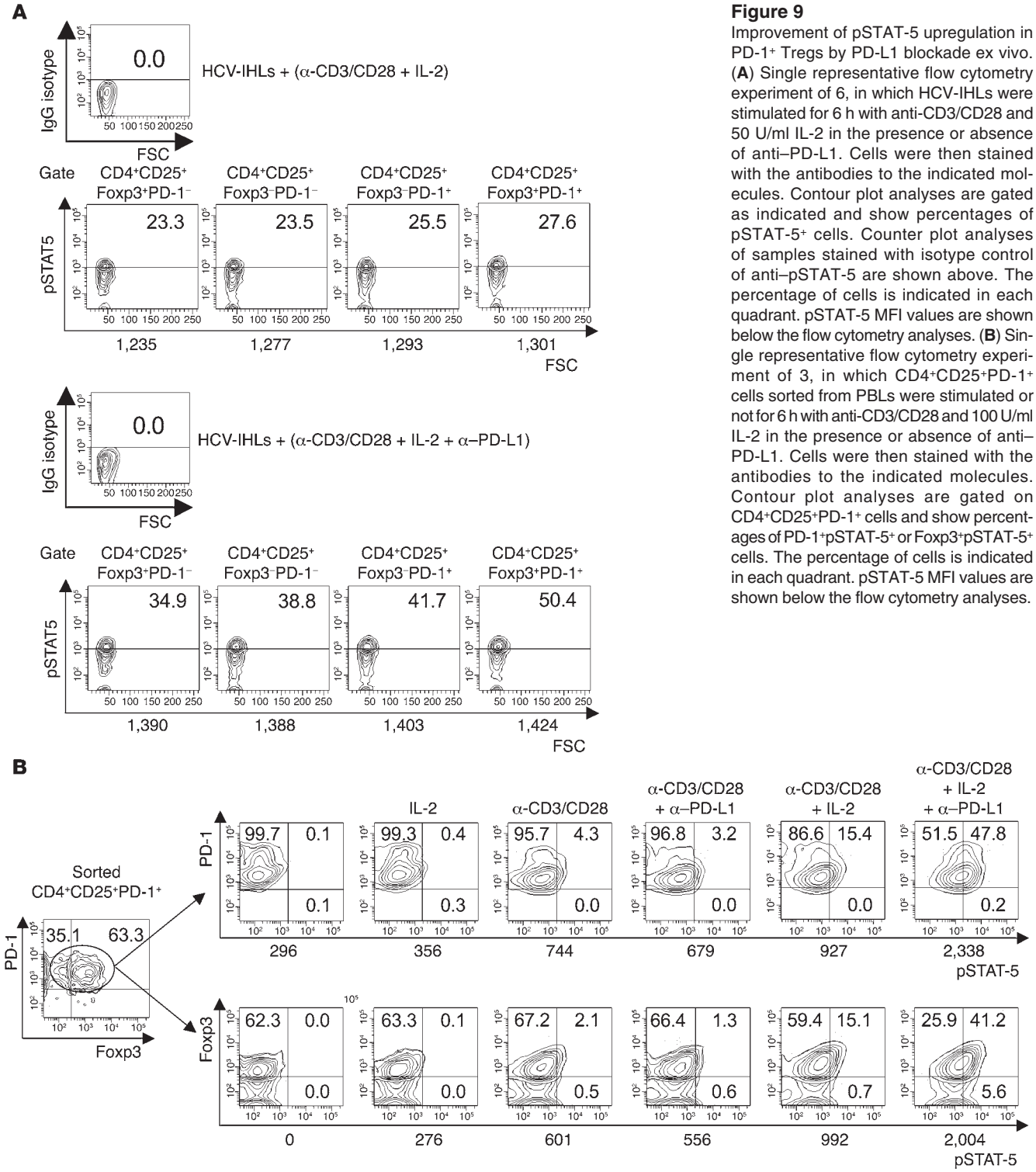

Figure 9

Improvement of pSTAT-5 upregulation in PD-1+ Tregs by PD-L1 blockade ex vivo. (**A**) Single representative flow cytometry experiment of 6, in which HCV-IHLs were stimulated for 6 h with anti-CD3/CD28 and 50 U/ml IL-2 in the presence or absence of anti–PD-L1. Cells were then stained with the antibodies to the indicated molecules. Contour plot analyses are gated as indicated and show percentages of pSTAT-5+ cells. Counter plot analyses of samples stained with isotype control of anti–pSTAT-5 are shown above. The percentage of cells is indicated in each quadrant. pSTAT-5 MFI values are shown below the flow cytometry analyses. (**B**) Single representative flow cytometry experiment of 3, in which CD4+CD25+PD-1+ cells sorted from PBLs were stimulated or not for 6 h with anti-CD3/CD28 and 100 U/ml IL-2 in the presence or absence of anti–PD-L1. Cells were then stained with the antibodies to the indicated molecules. Contour plot analyses are gated on CD4+CD25+PD-1+ cells and show percentages of PD-1+pSTAT-5+ or Foxp3+pSTAT-5+ cells. The percentage of cells is indicated in each quadrant. pSTAT-5 MFI values are shown below the flow cytometry analyses.

tion–induced apoptosis of Teffs (69). In this context, the inhibitory PD-1 effect on STAT-5 phosphorylation of Tregs may play a key role in controlling the suppression caused by IL-2 deprivation by limiting the expansion of IL-2–capturing Tregs. As a consequence, intrahepatic Teffs can escape from excessive expansion of Tregs, which have been recently suggested to exert IL-2 deprivation via cell-cell contact (69). However, our model does not exclude additional mechanisms by which the PD-L1–dependent pathway may interfere with Tregs by contrabalancing various mediators of Treg suppression (1–11, 70–72). Kinetics experiments showed that STAT-5 phosphorylation after IL-2 contact in vitro was notably more rapid in Tresps than in Tregs, whereas it increased and was sustained over time in Tregs more than in Tresps in the later phases. The interesting issue of whether Foxp3-induced anergy can

explain the requirement of more sustained IL-2 contact to initiate the STAT-5 phosphorylation cascade in Tregs may be the subject of further study. However, once appropriately rescued from anergy (i.e., via the capture of paracrine IL-2 in an inflamed tissue), $CD25^{hi}$ Tregs can capture higher IL-2 amounts than can $CD25^{lo}$ Teffs and induce more vigorous STAT-5 phosphorylation. In this scenario, the homeostasis between Treg and Teff expansion would be maintained by the higher expression of PD-1 on Tregs, which would prohibit exaggerated suppression of Teffs.

In conclusion, our results indicate that PD-L1–mediated inhibition limits the expansion of Tregs by controlling STAT-5 phosphorylation, thus providing a mechanism — which has not to our knowledge been described previously — by which Treg function can be contraregulated. Persisting pathogens are usually incompletely controlled by Teffs in primary infected individuals because of their capacities to generate escape mutants, to exert immunosuppressive effects, to induce Tregs, or to cause PD-1–dependent Teff exhaustion (32, 48, 51, 73–78). Our data suggest that under these circumstances, the balance between suppression (Foxp3) and contrasuppression (PD-1) may fine-tune Tregs in order to minimize the harmful responses without completely switching off those intended to limit excessive viral spread, and ultimately to maintain a long-lasting host/pathogen relationship. Studies are in progress to determine whether, on the other hand, predominant PD-1 contrasuppression of Tregs plays a key role in the degeneration leading to autoimmunity. Nevertheless, the inhibitory role of PD-1 in Tregs must be taken into account when targeting PD-1 or PD-L1 for therapeutic rationale, because such a strategy might result in boosting not only Teff responses, but also Treg-mediated immune suppression, which may have an advantageous role by inhibiting unwanted (e.g., autoreactive) responses.

Methods

HCV patients and HDs. We studied 65 HCV patients (Supplemental Table 1) and 30 HDs (age, 21–48 years; 21 males, 9 females) according to the ethical guidelines of the 1975 Declaration of Helsinki and a priori approval by the Institutional Review Boards of Sapienza Università di Roma and IRCCS Policlinico San Matteo di Pavia. In addition, 2 patients with chronic HCV infection (genotype 2c) showing a severe hepatitis reactivation were followed for a period of at least 50 d without receiving any treatment. Serum HCV-RNA levels and HCV genotype were determined by Versant HCV RNA 3.0 bDNA and INNO-LiPA, HCV II, respectively (Bayer Corp.). None of the patients were being treated with IFN-α with or without ribavirin, alternative antiviral therapies, or immunosuppressive therapies at the time of the study. Of the 65 HCV patients, 57 underwent percutaneous needle liver biopsy, part of which was processed for diagnostic and part for immunological analyses. Histology was graded as HAI, calculated as follows: periportal necrosis, intralobular necrosis, and portal inflammation were scored with values ranging 0–10, 0–4, and 0–4, respectively, and their sum provided the *grading* or inflammatory index; fibrosis was scored with a value ranging 0–4, providing the *staging* or fibrosis index; and the total score was calculated as grading plus staging (53).

Reagents. PE-cyanine 7–conjugated anti-CD4, peridinin-chlorophyll-protein complex–conjugated anti-CD25, and FITC-conjugated goat anti-rabbit IgG were from Caltag Laboratories. Allophycocyanin-conjugated anti-Foxp3 and PE-conjugated anti–PD-1 were from eBioscence. PE-conjugated anti–IL-2, FITC-conjugated anti-Ki67, FITC-conjugated anti-B7.1, control isotype–matched mAbs, and BD Cytofix/Cytoperm Kit were from BD Biosciences — Pharmingen. CFSE was from Invitrogen. Purified anti–PD-L1 mAb was from R&D Systems. Purified polyclonal rabbit anti–pSTAT-5 was from Cell Signalling. Dynabeads CD3/CD28 T Cell Expander (anti-CD3/CD28) was from Dynal Biotech. $CD4^+CD25^+$ Regulatory T Cell Isolation Kit was from Miltenyi Biotec. HCV-core and HCV-NS3 antigens were from ViroGen Co. and Biodesign International Inc., respectively. Brefeldin-A was from Sigma-Aldrich. Recombinant IL-2 was from Chiron. Cells producing the recombinant fusion protein constituted by CTLA-4 and human Ig were donated by F. Sallusto (Institute for Research in Biomedicine, Bellinzona, Switzerland; ref. 56). Complete medium was RPMI 1640 medium containing 5% fetal calf serum, 2 mM glutamine, 1% nonessential amino acids, 1% sodium pyruvate, and 50 μg/ml kanamycin from Invitrogen.

Cell preparation. PBLs and IHLs from liver biopsies were isolated as previously described (51, 73, 79). $CD4^+CD25^+$ T cells were purified from PBLs using the $CD4^+CD25^+$ Regulatory T Cell Isolation Kit (Miltenyi Biotec). Briefly, non-$CD4^+$ cells were depleted by separation over a MACS column (Miltenyi Biotec) after labeling with a cocktail of biotin-conjugated mAbs (anti-CD8, -CD14, -CD16, -CD19, -CD36, -CD123, -TCRγ/δ, and –Glycophorin A) and anti-Biotin MicroBeads (Miltenyi Biotec). Then, the enriched $CD4^+$ T cell fraction was conjugated with CD25 MicroBeads and separated using a MACS column. The unlabeled $CD4^+CD25^-$ T cell fraction was not retained in the column and obtained by collecting the effluent. Magnetically labeled $CD4^+CD25^+$ T cells were retained on the column and eluted after removal of the column from the magnetic field. Flow cytometry analysis using a FACSCanto flow cytometer (BD) and FACSDiva analysis software (version 5.0.3; BD) demonstrated 95%–99% and less than 5% $CD4^+CD25^+$ T cells in the labeled and unlabeled fraction, respectively. In addition, purified $CD4^+CD25^+$ cells were stained with PE-conjugated anti–PD-1 and then processed with FACSAria (BD) to sort $CD4^+CD25^+PD\text{-}1^+$ and $CD4^+CD25^+PD\text{-}1^-$ cells. Greater than 90% $PD\text{-}1^+$ cells were found in the positively sorted $PD\text{-}1^+CD4^+CD25^+$ cell population, and less than 3% were found in the $PD\text{-}1^-CD4^+CD25^+$ cells.

Surface and intracellular staining. The combination of differently labeled mAbs to surface molecules described above was used to stain PBLs or IHLs (51, 76, 77). After staining, cells were washed, fixed, and permeabilized using Cytofix/Cytoperm solution (BD Biosciences) at 4°C for 20 min, rewashed with Perm Wash Buffer (BD Biosciences), and stained at intracellular level with labeled mAbs to Foxp3 and Ki67 for 30 min at 4°C. When stained with unlabeled specific antibody to detect intracellular pSTAT-5, cells were washed and stained with the appropriate secondary labeled antibody. In selected experiments, cells that had been previously double stained with labeled mAbs to CD4 and CD25 were stimulated or not with anti-CD3/CD28 in the presence or absence of IL-2 (50 or 100 U/ml) for 6 h at 37°C. At the second hour, 5 μg/ml brefeldin-A was added. Cells were washed, fixed, permeabilized as described above, and stained at the intracellular level with labeled mAbs to Foxp3 and IL-2 for 30 min at 4°C. Negative controls were obtained by staining cells with irrelevant isotype-matched mAbs in each experiment. Stained cells were acquired with a FACSCanto flow cytometer and analyzed using FACSDiva software (BD).

Proliferation and suppression assays. Purified peripheral Tregs or Tresps, as well as sorted $PD\text{-}1^+$ or $PD\text{-}1^-$ Treg populations, were labeled with 1 μM CFSE for 10 min at 37°C, stopped with serum for 10 min at 37°C, washed with complete medium, and cultured alone (5×10^4) or cocultured at a 1:1 cell ratio in a 96-well plate in the presence or absence of different combinations of HCV-Ags/APCs, anti-CD3/CD28, 50 U/ml IL-2, blocking anti–PD-L1, CTLA-4/Ig, or isotype control mAb. Alternatively, Tregs and Tresps were cocultured in separated 96-transwell plates (Corning Inc.) and independently stimulated as described above. In selected experiments, in which we were able to obtain about 5×10^4 intrahepatic Tregs from pools of 4 liver biopsies, these cells were cultured alone or cocultured with CFSE-stained peripheral Tresps (isolated from 6 randomly selected HCV patients) at a 1:1 cell ratio as described above. After 6 d stimulation, cells were stained with

labeled mAbs to CD4, CD25, and Foxp3. In some experiments, PD-1$^+$ and PD-1$^-$ Treg populations were stimulated or not for 6 d with anti-CD3/CD28 and IL-2, in the presence or absence of anti–PD-L1, and stained with the labeled mAbs to CD4, CD25, PD-1, Foxp3, and Ki57 described above. Finally, cells were analyzed with a FACSCanto flow cytometer (BD).

Statistics. All statistical analyses were performed with both SPSS (version 11; SPSS Inc.) and Prism (version 4; GraphPad) software using Pearson's correlation test and nonparametric Mann-Whitney *U* test. Differences were considered significant at $P < 0.05$.

Acknowledgments

This work was supported by European Union financial supports; by Fondo per gli Investimenti della Ricerca di Base and Programmi di Ricerca scientifica di rilevante Interesse Nazionale, Ministero dell'Istruzione, dell'Università e della Ricerca projects; by Ministero della Sanità-Istituto Superiore di Sanità (Progetti AIDS); by Associazione Italiana per la Ricerca sul Cancro; by Fondazione Italiana Sclerosi Multipla; and by Contributo Regione Lazio per la realizzazione di opere strutturali ed iniziative sociali, culturali e sportive di carattere locale 2006.

Received for publication June 26, 2008, and accepted in revised form January 7, 2009.

Address correspondence to: Vincenzo Barnaba, Dipartimento di Medicina Interna, Sapienza Università di Roma, Policlinico "Umberto I," viale del Policlinico 155, 00161 Rome, Italy. Phone: 39-06-4453994; Fax: 39-06-49383333; E-mail: vincenzo.barnaba@uniroma1.it.

Vittorio Francavilla's present address is: Centro Nazionale AIDS, Istituto Superiore di Sanità, Rome, Italy.

1. Sakaguchi, S., Sakaguchi, N., Asano, M., Itoh, M., and Toda, M. 1995. Immunologic self-tolerance maintained by activated T cells expressing IL-2 receptor alpha-chains (CD25). Breakdown of a single mechanism of self-tolerance causes various autoimmune diseases. *J. Immunol.* **155**:1151–1164.
2. Takahashi, T., et al. 1998. Immunologic self-tolerance maintained by CD25+CD4+ naturally anergic and suppressive T cells: induction of autoimmune disease by breaking their anergic/suppressive state. *Int. Immunol.* **10**:1969–1980.
3. Baecher-Allan, C., Brown, J.A., Freeman, G.J., and Hafler, D.A. 2001. CD4+CD25high regulatory cells in human peripheral blood. *J. Immunol.* **167**:1245–1253.
4. Fontenot, J.D., Gavin, M.A., and Rudensky, A.Y. 2003. Foxp3 programs the development and function of CD4+CD25+ regulatory T cells. *Nat. Immunol.* **4**:330–336.
5. Hori, S., Nomura, T., and Sakaguchi, S. 2003. Control of regulatory T cell development by the transcription factor Foxp3. *Science.* **299**:1057–1061.
6. Khattri, R., Cox, T., Yasayko, S.A., and Ramsdell, F. 2003. An essential role for Scurfin in CD4+CD25+ T regulatory cells. *Nat. Immunol.* **4**:337–342.
7. Sakaguchi, S. 2004. Naturally arising CD4+ regulatory t cells for immunologic self-tolerance and negative control of immune responses. *Annu. Rev. Immunol.* **22**:531–562.
8. Shevach, E.M. 2002. CD4+ CD25+ suppressor T cells: more questions than answers. *Nat. Rev. Immunol.* **2**:389–400.
9. Fontenot, J.D., and Rudensky, A.Y. 2005. A well adapted regulatory contrivance: regulatory T cell development and the forkhead family transcription factor Foxp3. *Nat. Immunol.* **6**:331–337.
10. von Boehmer, H. 2005. Mechanisms of suppression by suppressor T cells. *Nat. Immunol.* **6**:338–344.
11. Ziegler, S.F. 2006. FOXP3: of mice and men. *Annu. Rev. Immunol.* **24**:209–226.
12. Malek, T.R., and Bayer, A.L. 2004. Tolerance, not immunity, crucially depends on IL-2. *Nat. Rev. Immunol.* **4**:665–674.
13. Malek, T.R., Yu, A., Vincek, V., Scibelli, P., and Kong, L. 2002. CD4 regulatory T cells prevent lethal autoimmunity in IL-2Rbeta-deficient mice. Implications for the nonredundant function of IL-2. *Immunity.* **17**:167–178.
14. Salomon, B., and Bluestone, J.A. 2001. Complexities of CD28/B7: CTLA-4 costimulatory pathways in autoimmunity and transplantation. *Annu. Rev. Immunol.* **19**:225–252.
15. Shimizu, J., Yamazaki, S., Takahashi, T., Ishida, Y., and Sakaguchi, S. 2002. Stimulation of CD25(+)CD4(+) regulatory T cells through GITR breaks immunological self-tolerance. *Nat. Immunol.* **3**:135–142.
16. Ruprecht, C.R., et al. 2005. Coexpression of CD25 and CD27 identifies FoxP3+ regulatory T cells in inflamed synovia. *J. Exp. Med.* **201**:1793–1803.
17. Liu, W., et al. 2006. CD127 expression inversely correlates with FoxP3 and suppressive function of human CD4+ T reg cells. *J. Exp. Med.* **203**:1701–1711.
18. Gavin, M.A., et al. 2007. Foxp3-dependent programme of regulatory T-cell differentiation. *Nature.* **445**:771–775.
19. Williams, L.M., and Rudensky, A.Y. 2007. Maintenance of the Foxp3-dependent developmental program in mature regulatory T cells requires continued expression of Foxp3. *Nat. Immunol.* **8**:277–284.
20. Schubert, L.A., Jeffery, E., Zhang, Y., Ramsdell, F., and Ziegler, S.F. 2001. Scurfin (FOXP3) acts as a repressor of transcription and regulates T cell activation. *J. Biol. Chem.* **276**:37672–37679.
21. Coffer, P.J., and Burgering, B.M. 2004. Forkhead-box transcription factors and their role in the immune system. *Nat. Rev. Immunol.* **4**:889–899.
22. Barthlott, T., et al. 2005. CD25+ CD4+ T cells compete with naive CD4+ T cells for IL-2 and exploit it for the induction of IL-10 production. *Int. Immunol.* **17**:279–288.
23. de la Rosa, M., Rutz, S., Dorninger, H., and Scheffold, A. 2004. Interleukin-2 is essential for CD4+CD25+ regulatory T cell function. *Eur. J. Immunol.* **34**:2480–2488.
24. Scheffold, A., Huhn, J., and Hofer, T. 2005. Regulation of CD4+CD25+ regulatory T cell activity: it takes (IL-)two to tango. *Eur. J. Immunol.* **35**:1336–1341.
25. Wildin, R.S., et al. 2001. X-linked neonatal diabetes mellitus, enteropathy and endocrinopathy syndrome is the human equivalent of mouse scurfy. *Nat. Genet.* **27**:18–20.
26. Brunkow, M.E., et al. 2001. Disruption of a new forkhead/winged-helix protein, scurfin, results in the fatal lymphoproliferative disorder of the scurfy mouse. *Nat. Genet.* **27**:68–73.
27. Gambineri, E., Torgerson, T.R., and Ochs, H.D. 2003. Immune dysregulation, polyendocrinopathy, enteropathy, and X-linked inheritance (IPEX), a syndrome of systemic autoimmunity caused by mutations of FOXP3, a critical regulator of T-cell homeostasis. *Curr. Opin. Rheumatol.* **15**:430–435.
28. Miura, Y., et al. 2004. Association of Foxp3 regulatory gene expression with graft-versus-host disease. *Blood.* **104**:2187–2193.
29. Balandina, A., Lecart, S., Dartevelle, P., Saoudi, A., and Berrih-Aknin, S. 2005. Functional defect of regulatory CD4(+)CD25+ T cells in the thymus of patients with autoimmune myasthenia gravis. *Blood.* **105**:735–741.
30. Huan, J., et al. 2005. Decreased FOXP3 levels in multiple sclerosis patients. *J. Neurosci. Res.* **81**:45–52.
31. Wan, Y.Y., and Flavell, R.A. 2007. Regulatory T-cell functions are subverted and converted owing to attenuated Foxp3 expression. *Nature.* **445**:766–770.
32. Belkaid, Y. 2007. Regulatory T cells and infection: a dangerous necessity. *Nat. Rev. Immunol.* **7**:875–888.
33. Sharpe, A.H., Wherry, E.J., Ahmed, R., and Freeman, G.J. 2007. The function of programmed cell death 1 and its ligands in regulating autoimmunity and infection. *Nat. Immunol.* **8**:239–245.
34. Keir, M.E., Francisco, L.M., and Sharpe, A.H. 2007. PD-1 and its ligands in T-cell immunity. *Curr. Opin. Immunol.* **19**:309–314.
35. Ha, S.J., et al. 2008. Enhancing therapeutic vaccination by blocking PD-1-mediated inhibitory signals during chronic infection. *J. Exp. Med.* **205**:543–555.
36. Day, C.L., et al. 2006. PD-1 expression on HIV-specific T cells is associated with T-cell exhaustion and disease progression. *Nature.* **443**:350–354.
37. Trautmann, L., et al. 2006. Upregulation of PD-1 expression on HIV-specific CD8+ T cells leads to reversible immune dysfunction. *Nat. Med.* **12**:1198–1202.
38. Urbani, S., et al. 2006. PD-1 expression in acute hepatitis C virus (HCV) infection is associated with HCV-specific CD8 exhaustion. *J. Virol.* **80**:11398–11403.
39. Maier, H., Isogawa, M., Freeman, G.J., and Chisari, F.V. 2007. PD-1:PD-L1 interactions contribute to the functional suppression of virus-specific CD8+ T lymphocytes in the liver. *J. Immunol.* **178**:2714–2720.
40. Boni, C., et al. 2007. Characterization of hepatitis B virus (HBV)-specific T-cell dysfunction in chronic HBV infection. *J. Virol.* **81**:4215–4225.
41. Penna, A., et al. 2007. Dysfunction and functional restoration of HCV-specific CD8 responses in chronic hepatitis C virus infection. *Hepatology.* **45**:588–601.
42. Golden-Mason, L., et al. 2007. Upregulation of PD-1 expression on circulating and intrahepatic hepatitis C virus-specific CD8+ T cells associated with reversible immune dysfunction. *J. Virol.* **81**:9249–9258.
43. Radziewicz, H., et al. 2007. Liver-infiltrating lymphocytes in chronic human hepatitis C virus infection display an exhausted phenotype with high levels of PD-1 and low levels of CD127 expression. *J. Virol.* **81**:2545–2553.
44. Raimondi, G., Shufesky, W.J., Tokita, D., Morelli, A.E., and Thomson, A.W. 2006. Regulated compartmentalization of programmed cell death-1 discriminates CD4+CD25+ resting regulatory T cells from activated T cells. *J. Immunol.* **176**:2808–2816.
45. Scott-Browne, J.P., et al. 2007. Expansion and function of Foxp3-expressing T regulatory cells during tuberculosis. *J. Exp. Med.* **204**:2159–2169.
46. Sharma, M.D., et al. 2007. Plasmacytoid dendritic cells from mouse tumor-draining lymph nodes directly activate mature Tregs via indoleamine 2,3-dioxygenase. *J. Clin. Invest.* **117**:2570–2582.
47. Lauer, G.M., and Walker, B.D. 2001. Hepatitis C

virus infection. *N. Engl. J. Med.* **345**:41–52.
48. Dustin, L.B., and Rice, C.M. 2007. Flying under the radar: the immunobiology of hepatitis C. *Annu. Rev. Immunol.* **25**:71–99.
49. Gavin, M.A., et al. 2006. Single-cell analysis of normal and FOXP3-mutant human T cells: FOXP3 expression without regulatory T cell development. *Proc. Natl. Acad. Sci. U. S. A.* **103**:6659–6664.
50. Lanzavecchia, A., and Sallusto, F. 2000. Dynamics of T lymphocyte responses: intermediates, effectors, and memory cells. *Science.* **290**:92–97.
51. Accapezzato, D., et al. 2004. Hepatic expansion of a virus-specific regulatory CD8(+) T cell population in chronic hepatitis C virus infection. *J. Clin. Invest.* **113**:963–972.
52. Thornton, A.M., Piccirillo, C.A., and Shevach, E.M. 2004. Activation requirements for the induction of CD4+CD25+ T cell suppressor function. *Eur. J. Immunol.* **34**:366–376.
53. Desmet, V.J., Gerber, M., Hoofnagle, J.H., Manns, M., and Scheuer, P.J. 1994. Classification of chronic hepatitis: diagnosis, grading and staging. *Hepatology.* **19**:1513–1520.
54. Ward, S.M., et al. 2007. Quantification and localisation of FOXP3+ T lymphocytes and relation to hepatic inflammation during chronic HCV infection. *J. Hepatol.* **47**:316–324.
55. Butte, M.J., Pena-Cruz, V., Kim, M.J., Freeman, G.J., and Sharpe, A.H. 2008. Interaction of human PD-L1 and B7-1. *Mol. Immunol.* **45**:3567–3572.
56. Lane, P., Gerhard, W., Hubele, S., Lanzavecchia, A., and McConnell, F. 1993. Expression and functional properties of mouse B7/BB1 using a fusion protein between mouse CTLA4 and human gamma 1. *Immunology.* **80**:56–61.
57. O'Shea, J.J., Gadina, M., and Schreiber, R.D. 2002. Cytokine signaling in 2002: new surprises in the Jak/Stat pathway. *Cell.* **109**(Suppl):S121–S131.
58. Shuai, K., and Liu, B. 2003. Regulation of JAK-STAT signalling in the immune system. *Nat. Rev. Immunol.* **3**:900–911.
59. Antov, A., Yang, L., Vig, M., Baltimore, D., and Van Parijs, L. 2003. Essential role for STAT5 signaling in CD25+CD4+ regulatory T cell homeostasis and the maintenance of self-tolerance. *J. Immunol.* **171**:3435–3441.
60. Passerini, L., et al. 2008. STAT5-signaling cytokines regulate the expression of FOXP3 in CD4+CD25+ regulatory T cells and CD4+CD25- effector T cells. *Int. Immunol.* **20**:421–431.
61. Rumi, M.G., et al. 2005. Hepatitis C reactivation in patients with chronic infection with genotypes 1b and 2c: a retrospective cohort study of 206 untreated patients. *Gut.* **54**:402–406.
62. Ebinuma, H., et al. 2008. Identification and in vitro expansion of functional antigen-specific CD25+ FoxP3+ regulatory T cells in hepatitis C virus infection. *J. Virol.* **82**:5043–5053.
63. Barnaba, V., et al. 1989. Recognition of hepatitis B virus envelope proteins by liver-infiltrating T lymphocytes in chronic HBV infection. *J. Immunol.* **143**:2650–2655.
64. Benvenuto, R., et al. 1991. Enhanced production of interferon-gamma by T lymphocytes cloned from rejected kidney grafts. *Transplantation.* **51**:887–890.
65. Barnaba, V., et al. 1994. Selective expansion of cytotoxic T lymphocytes with a CD4+CD56+ surface phenotype and a T helper type 1 profile of cytokine secretion in the liver of patients chronically infected with Hepatitis B virus. *J. Immunol.* **152**:3074–3087.
66. Nuti, S., et al. 1998. Dynamics of intra-hepatic lymphocytes in chronic hepatitis C: enrichment for Valpha24+ T cells and rapid elimination of effector cells by apoptosis. *Eur. J. Immunol.* **28**:3448–3455.
67. Matzinger, P. 2007. Friendly and dangerous signals: is the tissue in control? *Nat. Immunol.* **8**:11–13.
68. Furtado, G.C., Curotto de Lafaille, M.A., Kutchukhidze, N., and Lafaille, J.J. 2002. Interleukin 2 signaling is required for CD4(+) regulatory T cell function. *J. Exp. Med.* **196**:851–857.
69. Pandiyan, P., Zheng, L., Ishihara, S., Reed, J., and Lenardo, M.J. 2007. CD4+CD25+Foxp3+ regulatory T cells induce cytokine deprivation-mediated apoptosis of effector CD4+ T cells. *Nat. Immunol.* **8**:1353–1362.
70. Read, S., et al. 2006. Blockade of CTLA-4 on CD4+CD25+ regulatory T cells abrogates their function in vivo. *J. Immunol.* **177**:4376–4383.
71. Li, R., et al. 2007. Enhanced engagement of CTLA-4 induces antigen-specific CD4+CD25+Foxp3+ and CD4+CD25- TGF-beta 1+ adaptive regulatory T cells. *J. Immunol.* **179**:5191–5203.
72. Deaglio, S., et al. 2007. Adenosine generation catalyzed by CD39 and CD73 expressed on regulatory T cells mediates immune suppression. *J. Exp. Med.* **204**:1257–1265.
73. Barnaba, V., Franco, A., Alberti, A., Benvenuto, R., and Balsano, F. 1990. Selective killing of hepatitis B envelope antigen-specific B cells by class I-restricted, exogenous antigen-specific T lymphocytes. *Nature.* **345**:258–260.
74. Tortorella, D., Gewurz, B.E., Furman, M.H., Schust, D.J., and Ploegh, H.L. 2000. Viral subversion of the immune system. *Annu. Rev. Immunol.* **18**:861–926.
75. Sacks, D., and Sher, A. 2002. Evasion of innate immunity by parasitic protozoa. *Nat. Immunol.* **3**:1041–1047.
76. Francavilla, V., et al. 2004. Subversion of effector CD8+ T cell differentiation in acute hepatitis C virus infection: exploring the immunological mechanisms. *Eur. J. Immunol.* **34**:427–437.
77. Accapezzato, D., et al. 2004. Subversion of effector CD8+ T cell differentiation in acute hepatitis C virus infection: the role of the virus. *Eur. J. Immunol.* **34**:438–446.
78. Loureiro, J., and Ploegh, H.L. 2006. Antigen presentation and the ubiquitin-proteasome system in host-pathogen interactions. *Adv. Immunol.* **92**:225–305.
79. Prezzi, C., et al. 2001. Virus-specific CD8(+) T cells with type 1 or type 2 cytokine profile are related to different disease activity in chronic hepatitis C virus infection. *Eur. J. Immunol.* **31**:894–906.